Three-dimensional configuration of orientated fibers as guidance structures for cell migration and axonal growth

Andreas Kriebel, Muhammad Rumman, Miriam Scheld, Dorothee Hodde, Gary Brook, Jörg Mey

Angaben zur Veröffentlichung / Publication details:

Kriebel, Andreas, Muhammad Rumman, Miriam Scheld, Dorothee Hodde, Gary Brook, and Jörg Mey. 2013. "Three-dimensional configuration of orientated fibers as guidance structures for cell migration and axonal growth." *Journal of Biomedical Materials Research Part B: Applied Biomaterials* 102 (2): 356–65. https://doi.org/10.1002/jbm.b.33014.

Three-dimensional configuration of orientated fibers as guidance structures for cell migration and axonal growth

Andreas Kriebel,[1,2] Muhammad Rumman,[1] Miriam Scheld,[1] Dorothee Hodde,[3,4] Gary Brook,[2,3,4] Jörg Mey[1,2,5]

[1]Institut für Biologie II, RWTH Aachen, Germany
[2]EURON Graduate School of Neuroscience, Maastricht University, Netherlands
[3]Institut für Neuropathologie, Universitätsklinikum Aachen, Germany
[4]Jülich-Aachen Research Alliance – Translational Brain Medicine (JARA Brain), Germany
[5]Laboratorio de Regeneración Nerviosa, Hospital Nacional de Parapléjicos, Toledo, Spain

Abstract: Peripheral nerve injuries can be surgically repaired by suturing the transected nerve stumps or, in case of larger lesions, by the transplantation of an autologous nerve graft. To avoid donor site morbidity, the development of artificial implants is desired. Clinically, hollow conduits have been used for this purpose but are inferior to the autograft because they lack internal guidance cues for Schwann cells and regenerating axons. In this article, we describe the design of a three-dimensional (3D) scaffold consisting of parallel fibers embedded in a collagen matrix. For this purpose, an electrospinning device was developed to produce and manipulate a 3D array of aligned poly(ε-caprolactone) (PCL) microfibers. This fiber array was then incorporated into biodegradable PCL tubes to serve as artificial nerve bridges. Using primary cultures of embryonic chicken dorsal root ganglia, we show that PCL microfibers in the 3D matrix of our composite scaffold guide the direction of Schwann cell migration and axonal growth. © 2013 Wiley Periodicals, Inc. J Biomed Mater Res Part B: Appl Biomater, 102B: 356–365, 2014.

Key Words: peripheral nerve, regeneration, biomaterials, electrospinning, artificial implants, extracellular matrix, growth factors

INTRODUCTION

Peripheral nerve (PN) lesions can be surgically repaired by suturing the proximal and distal nerve stumps together. In these cases, axons regenerating from injured motor, sensory, and autonomic neurons are able to grow within the scaffolds of Schwann cells and extracellular matrix (ECM) of the injured nerve.[1] When PN injuries result in larger gaps between transected nerve ends, these have to be bridged, for instance, by transplanting a sensory nerve from the same patient. Unfortunately, this approach is functionally successful only in about half of the patients and has other disadvantages, such as sensory loss at the donor site and a limited availability of transplant material.[2] Currently, much research is therefore devoted to developing artificial nerve conduits that can replace autologous transplants.[2–4]

For clinical use in humans, only simple tubular conduits have so far been approved in the United States and Europe.[3] The majority of animal experiments is also based on the design of the hollow tube. Because axons grow on surfaces and must be guided toward their peripheral target, better results are expected if internal structures could support axonal growth and induce colonization with host-derived Schwann cells, which are required for trophic support and the subsequent remyelination of regenerated nerve fibers.[5] Recent advances in the design of artificial nerve implants therefore focus on topographical features that guide axonal regeneration and cell migration. Basic design strategies for nerve bridges with internal guidance structures are based on (1) large interior channels to separate individual fiber fascicles,[6,7] (2) scaffolds with many longitudinally orientated pores,[8,9] or (3) parallel aligned polymer fibers produced by melt extrusion[10,11] or electrospinning[12–14] (Figure 1).

Our approach is based on electrospinning of the biodegradable polyester poly(ε-caprolactone) (PCL) using two separated target electrodes, such that parallel fibers accumulate between them.[13,15] The resulting microfibers have been shown to be excellent growth substrates for glial cells and axons of sensory neurons.[16,17] Given successful *in vitro* tests of several two-dimensional growth substrates a major challenge in scaffold design consists in the construction of three-dimensional (3D) structures that can be implanted *in vivo*. In this study, we describe a technique for 3D spinning

Correspondence to: J. Mey (e-mail: jmey@sescam.jccm.es)
Contract grant sponsor: Deutsche Forschungsgemeinschaft; contract grant number: ME 1261/11 (to J.M.)

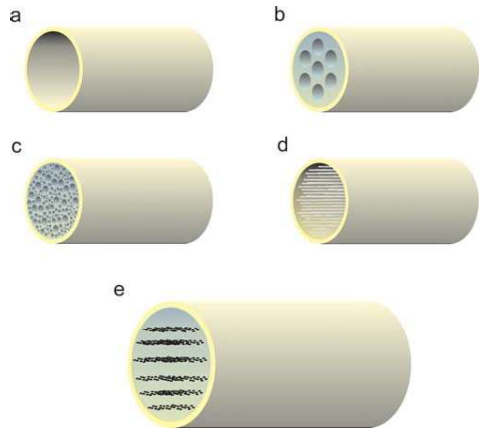

FIGURE 1. Conduit design for artificial nerve guides. (a) Empty tube used for bridging gaps between proximal and distal nerve stumps, used in most experiments so far; (b) tubular implant with multiple intraluminal channels (e.g., Refs. 7 and 20); (**c**) tube filled with an internal matrix structured by longitudinally oriented pores or channels (e.g., Ref. 34); (d) aligned polymer fibers as longitudinal guidance structures (e.g., Refs. 10 and 14); (**e**) present construct consisting of 3D aligned PCL fibers embedded in layers of collagen gel. [Color figure can be viewed in the online issue, which is available at wileyonlinelibrary.com.]

of parallel microfibers, their embedding in collagen gels, and incorporation in biodegradable PCL tubes. The biocompatibiliy of the resulting 3D scaffold was investigated using dorsal root ganglia (DRG) explants.

MATERIALS AND METHODS

Electrospinning of three-dimensional fiber arrays

Solvents and PCL used for electrospinning were purchased from Sigma-Aldrich Chemie GmbH (Munich, Germany). Electrospinning was performed with 8 wt % and 12 wt % PCL ($M_n = 70{,}000$–$90{,}000$ g/mol) dissolved in chloroform/methanol (3:1). Unless otherwise indicated, data are reported for fibers made from 12% PCL. The spinneret consisted of a syringe with a 20G flat tipped needle connected to a metal disc with 90 mm diameter. After various target electrodes had been tested, the standard target configuration consisted of two opposing aluminum bars with a distance of 18 mm between them. These were mounted on a tapered base, which was connected with its narrow end to a grounded metal disc [Figure 2(a)]. Of the different target devices, all made of aluminum [Figure 2(b–e)], a stair case-like target was used for spinning of 3D fiber arrays (different sizes were successfully tested, e.g., 12 steps, 20 mm breadth, 1 mm step size; five steps, 13 mm breadth, 1 mm step size; [Figures 2(d,e) and 3(a)]). Standard spinning conditions were 17 kV, with 20 cm distance to the collector without mechanical ejection of the polymer solution by a syringe pump resulting in a feed rate of about 0.5 mL/h. However, depending on ambient conditions the distance between spinneret and target was adjusted between 17 and 20 cm to give best results. For spinning of one batch of fibers we applied the voltage for approximately 30 s to the spinneret. To handle the three-dimensional array of fibers after spinning, the bars were attached to a U-shaped frame before disassembling it from the base. To visualize electrospun fibers with fluorescence microscopy, the lipophilic dye DiI [Molecular Probes, D3911, 75 μL DiI/DMSO (1/1000) in 20 mL] was added to the PCL solution.

Physical characterization of fiber arrays

Electrospun fibers suspended on the targets were examined with a Leica TCS SP2 confocal microscope (Leica Microsystems GmbH, Wetzlar, Germany). For documentation of alignment and density of the fiber arrays we produced image stacks from the upper most fiber plane reaching 2 mm down into the lowest fiber plane. The image stacks were processed for further analysis using Image J software. For evaluation of fiber density, we divided a stack into five bins of 400 μm, made a projection of all images in one bin and counted the number of fibers crossing the midline. For assessing fiber alignment, the mean direction of all fibers in a stack was determined and the deviation angles of the individual fibers were plotted. The standard deviation (SD) of deviation angles was calculated using MATLAB.

Fiber diameter was determined by sputter coating the samples with 30 nm gold and performing scanning electron microscopy using a FEI/Philips XL30 FEG ESEM with a 10-kV electron beam. Using high magnification (5000×) images of single fibers we averaged the thickness of each fiber from five positions within an image. Mean fiber thickness and

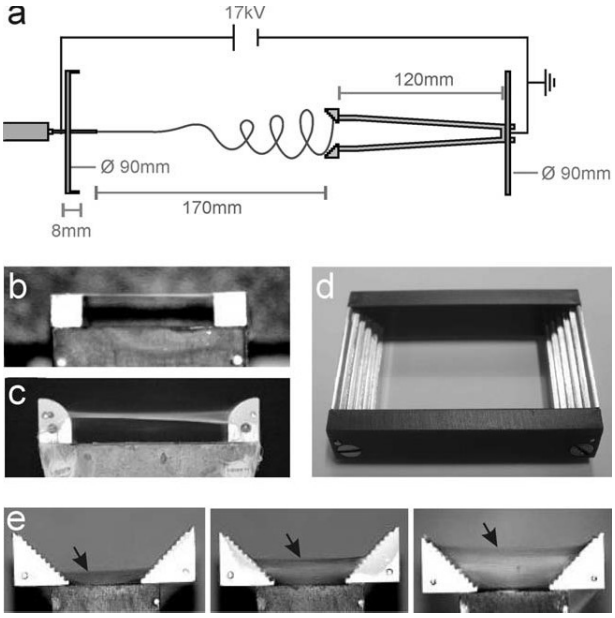

FIGURE 2. Electrospinning setup for the collection of 3D fiber arrays. (a) Schematic diagram of the spinning device consisting of a syringe, 20 gauge needle connected with a metal plate (spinneret), high voltage power supply, and grounded collection target, which is mounted on a conducting v-shaped base likewise connected to a metal plate. (b–e) Photos of different target designs to illustrate accumulation of parallel fibers. Two parallel bars (b) resulted in a single layer of parallel fibers accumulating on the upper edge. Substituting edged bars with a curvature allowed (c) accumulation on a slightly wider depth on the target. The best target for 3D-spinning is characterized by a stepped design (d) resulting in a sequential accumulation of fibers from bottom to the top edge (e, arrows).

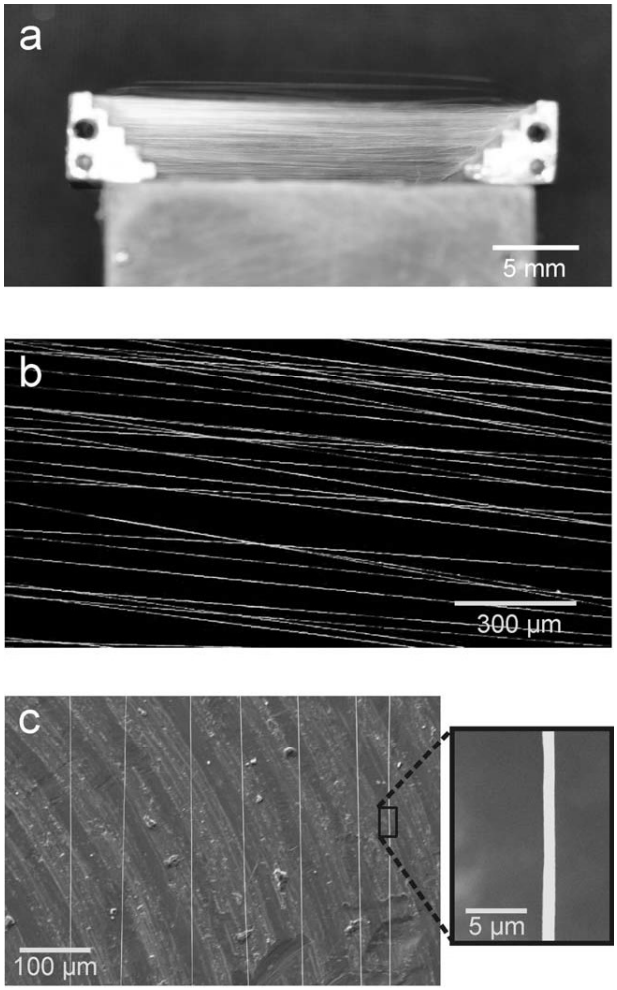

FIGURE 3. Three-dimensional arrays of parallel fibers. (a) Electrospun fibers suspended in a step target are shown from the side. (b) Projection of a 400-µm confocal scan from above demonstrates the parallel alignment of the fibers. (c) SEM image of fibers with 200-fold and 5000-fold magnification. High magnification photos were used to determine the fiber diameters (fiber seen as a vertical line in the inset; 808 ± 175 nm, mean ± SD).

standard error (SEM) were calculated from 23 fibers of five different samples.

Inserting the 3D fiber arrays into a conduit

For biological testing, the electrospun fibers were inserted in gels that consisted of type I collagen. For the matrix, we prepared a 2.4 mg/mL solution of rat tail collagen I (Life Technologies, A1048301) according to the manufacturer's protocol. In brief, one part 10× basal medium Eagle was added to eight parts rat tail collagen I solution. We neutralized the pH with 1*M* NaOH and then filled up to 10 parts with distilled water (DRG cultures) or with cell suspension to obtain 10^6 cells/mL. To prevent premature gelation, the collagen solution was kept on ice during the whole procedure. To fabricate composites of collagen and PCL fibers, a drop of 50 µL collagen solution was applied onto a poly-L-lysine coated cover slip. Using a U-shaped frame to hold the target electrodes the fiber array was deposited into the collagen solution and detached from the frame using hot forceps. To induce gelation, the composites were placed in an incubator for 30–40 min at 37°C and 95% humidity. This step could be repeated several times to incorporate additional layers of fibers.

For manufacturing implantable tubes to be filled with the composite of gel and fibers, porous, biodegradable PCL tubes were made by dip coating. Crystalline NaCl was ground to fine powder in a mortar and was mixed with an equal amount (wt) of a 12% PCL-solution in chloroform/methanol (3:1). Steel wires of 2 mm diameter were repeatedly dipped into the NaCl/PCL suspension to produce conduits of 1–2 cm length and 500 µm wall thickness (for a final construct of 1.5 cm). The surface was leveled after 1 min drying at RT. After another 5 h of drying, the conduits were removed from the wires and transferred to a Petri dish with stirred deionized water for 24 h to dissolve the NaCl.[18] Water was changed twice. Conduits were cut lengthwise in half and filled with gel/fiber stacks as described above for glass cover slips. Subsequently, half-tubes were resealed using the PCL solution and equilibrated with cell culture medium. All steps were performed under sterile conditions. The thickness of the tube wall was determined with scanning electron miscroscopy.

Cell and organ culture

All cell culture reagents were purchased from Life Technologies GmbH (Darmstadt, Germany). Before the experiments, astrocytoma cells (U373) were grown in Dulbecco's modified Eagle medium (DMEM) with Glutamax and enriched with 10% fetal calf serum (FCS) and 0.2% penicillin/streptomycin at 37°C, 5% CO_2. The culture medium was changed every second day and cultures were split twice a week. For the experiments, cells were washed with phosphate buffered saline (PBS) and detached from the surface of the culture flask using 0.25% trypsin/ethylenediaminetetraacetic acid (EDTA). After trypsination was stopped by adding 5 mL serum containing medium, cells were centrifuged and resuspended in culture medium. Cell numbers were determined using a Thoma chamber.

For organ cultures, we dissected DRG from 10-day-old chicken embryos. The embryos were decapitated and the skin removed. Accessing from the dorsal side, sharp forceps were inserted close to the lumbar vertebral column. By opening the forceps the hind limb could then be separated from the torso. The DRG, remaining on the inside of the thigh, were removed and collected in cold, sterile PBS, where they were kept until being transferred to the collagen matrix (< 30 min) and before adding of the PCL-fibers. After gel formation, the samples were placed in a 24-well plate with 1 mL culture medium and incubated at 37°C and 5% CO_2 for 6 (single cells) or 7 days (DRG). The medium was changed once after 3 days.

The biological compatibility of the complete conduits was also tested with DRG cultures. After coating the inner side of the longitudinally sectioned half-conduits with poly-L-lysine, several layers of collagen and PCL-fibers were

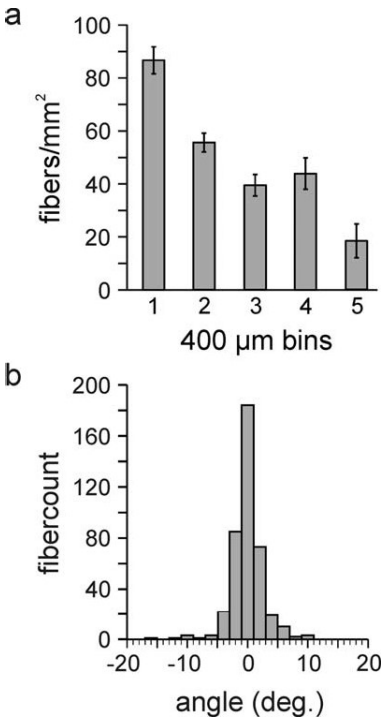

FIGURE 4. Quantitative characterization of the 3D fiber array. (a) Fiber density was determined from sequential confocal scans of 400 µm thickness through the fiber arrays suspended in the target frame (mean ± SEM, $n = 3$ targets). The fiber density decreases from top to bottom with the bottom layer still containing more than 18 fibers/mm^2. (b) The histogram depicts variability of fiber orientation as individual deviation from the mean orientation ($n = 559$ fibers from six samples. Angular standard deviation is 2.46°).

added together with a DRG explant. To allow microscopic evaluation, we sealed the surface with a poly-L-lysin coated cover slip and transferred the assembly upside down to a culture well, where culture media could only enter through the wall or the endings of the conduit. After 30 min gelation at 37°C we added 1 mL of culture medium to the well. The culture was maintained for 7 days with medium change once after 3 days *in vitro*. Axonal growth and cell migration was investigated in whole mounts.

Immunocytochemistry

Samples were fixed 1 h with cold 4% paraformaldehyde/phosphate buffer, rinsed with PBS and blocked with 1% bovine serum albumin, 4% normal goat serum and 0.1% TritonX-100 in PBS for 1 h. Incubation with the primary antibody [either 1/500 rabbit-anti-S100 (Sigma-Aldrich, Munich, Germany, S2644) or 1/500 rabbit-anti-NF200 (Sigma-Aldrich, N4142)] was performed over night at 4°C in blocking solution. Incubation with secondary antibody, Alexa Fluor 488 goat-anti-rabbit (Life Technologies GmbH, Darmstadt, Germany, A11008), 1/500 in blocking solution, was done for 1 h at room temperature followed by nuclear staining with 4',6-diamidino-2-phenylindole (DAPI, 1:5000) for 10 min. Negative controls were performed without primary antibodies. Samples were placed upside down on object slides using Fluoprep (Biomerieux) to stabilize fluorochromes.

Fluorescence microscopy

Images of the U373 astrocytoma cell cultures were captured using a Leica TCS SP2 confocal microscope and were further processed using Image J software. Cell migration and axonal outgrowth from DRG were analyzed with a Leica DM5000B epifluorescence microscope using filter cubes L5, N2.1 and A4 for Alexa Fluor 488, DiI and DAPI nuclear staining. Photos were recorded with a Leica DFC350 FX digital camera. Composite pictures of entire DRG and all outgrowing cells and axons were assembled by means of a Leica DMI6000 microscope with LASAF software. Individual cells and their interaction with PCL fibers were imaged using Leica TCS-SP5 confocal microscopy and further processed using Image J.

Quantification of Schwann cell migration and axonal growth

On composite photographs of DRG four tangents were drawn to the edges of the DRG in parallel and orthogonal to the fiber direction or, in case of the controls, horizontal and vertical with respect to the photographic frame. For cell migration, we measured the distance between the farthest cell body and the corresponding tangent. For axonal outgrowth, we counted the number of visible axonal endings and measured the distance between the 10% longest axons and the corresponding tangent. In the statistical analysis the individual DRG were considered as independent samples. Conditions were compared using Student's *t*-test, calculated with MATLAB.

RESULTS

Electrospinning of parallel fibers in a 3D configuration

The configuration of the fiber array produced with electrospinning depends on the geometry of the target which is used. Although a simple plate target results in a mat of non-oriented fibers, parallel fiber alignment can be obtained with targets consisting of a rotating drum or two parallel bars. Using the latter design, we collected PCL fibers that were suspended in the air between the two target bars [Figure 2(a)]. Fibers were aligned in parallel but formed one layer as they attached to the upper edge of the bars [Figure 2(b)]. To achieve a 3D array of the accumulating fibers, various target configurations were tested by modifying the bars. For instance, replacing the sharp edges with a rounder curvature led to the accumulation of fibers on a slightly wider area of the target, yet the distribution was not easy to control and was frequently different between the left and right bar [Figure 2(c)]. Taking advantage of the fact that the fibers tend to accumulate on edges, where electric field lines converge, we designed step-like targets with multiple edges facing each other [Figure 2(d)]. On this kind of target, the accumulation of fibers starts at the lowest edges. With increasing density as fibers accumulate on these edges, electrostatic repulsion between them forced further fiber accumulation towards the next higher steps. In this way, a consecutive accumulation of fibers from bottom to top was achieved [Figure 2(e)] resulting in a 3D configuration of PCL fibers. A view from the side of a 3D fiber array spun

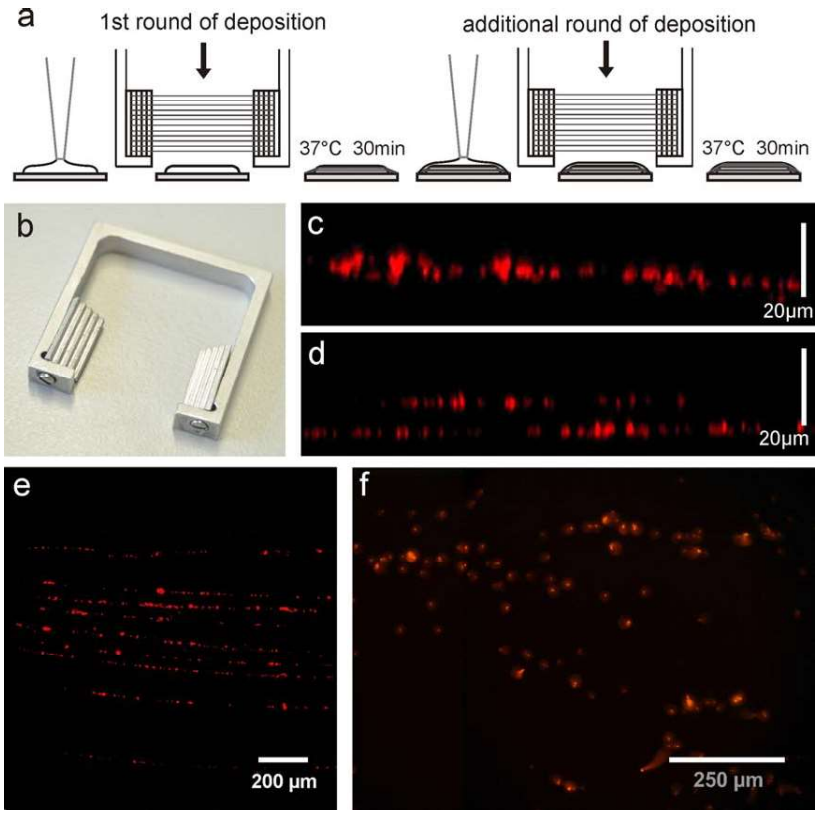

FIGURE 5. Embedding of 3D fiber stacks in collagen. (a) Schematic drawing of the embedding process. The collagen solution is applied onto a poly(lysine)-coated coverslip. Subsequently, fibers are dipped into the collagen solution and detached from the frame using hot forceps. Gelling was induced by incubation of the composite at 37°C for 30 min. To add fiber layers, the process was repeated several times. (b) For handling of the fiber stacks a U-shaped frame was used to keep the two parts of the target in place when detached from the base. (c–e) Arrangement of fiber stacks in the collagen gel shown in cross section after one (c), two (d), and 10 (e) rounds of deposition. (f) One single 3D array of PCL fibers was maintained in a gelatin gel which was cast over the fibers suspended between the target electrodes. [Color figure can be viewed in the online issue, which is available at wileyonlinelibrary.com.]

onto the final version of the target is shown in Figure 3(a). Microscopic evaluation of fluorescently labeled fibers [Figure 3(b)] and SEM visualization [Figure 3(c)] demonstrated the degree of their alignment.

Characterization of electrospun 3D PCL-fiber arrays

To quantitatively characterize the fiber arrays, the fiber density at different depths inside the array was binned [bin 1 to 5; Figure 4(a)]. The fiber density decreased from the top to the bottom of the 3D array, with the highest and lowest fiber density, 86.7 ± 5.1 fibers/mm^2 (area of cross section, $n = 5$ fiber stacks, mean $\pm$ SEM) and 18.3 ± 6.4 fibers/mm^2 in the first and last bin, respectively (ANOVA $p < 0.005$; $F = 8.00$; df $= 4$). The mean fiber density was 48.8 ± 4.5 fibers/mm^2.

To assess fiber alignment, we determined the direction of the individual fibers, calculated the mean orientation of all fibers and for every fiber its deviation angle from the mean orientation [Figure 4(b)]. The alignment of electrospun fibers was high, as fiber angles showed a narrow Gaussian distribution with around 70% of the fibers deviating less than 2.5° from the mean fiber orientation ($n = 559$ fibers; SD = 2.46°). Only about 1% of all measured fibers deviated more than 10° from the mean. The maximum deviation was 15°.

Fiber diameters were determined on the basis of scanning electron microscopy photos [Figure 3(c)]. As described previously,[19] fiber diameter was dependent on the PCL concentration of the spinning solution used. A concentration of 8% PCL resulted in a fiber diameter of 660 ± 190 nm (mean $\pm$ SEM). By raising the concentration to 12%, the fiber diameter was increased to 808 ± 175 nm ($p < 0.05$; compared by student's t-test).

Suspension and manipulation of 3D fiber arrays in biocompatible gels

The 3D arrays of PCL fibers were embedded into a collagen matrix by inserting the fibers into the gel [Figure 5(a)]. To handle the 3D fiber stacks for this purpose, electrodes were fixed to a metal frame [Figure 5(b)] and detached from the spinning setup with the suspended fibers between them. The embedding caused some compression of the array thereby increasing the fiber density.

To achieve larger 3D stacks that were not limited by the size of the electrospinning targets, this procedure could be repeated several times by stacking alternate layers of fiber

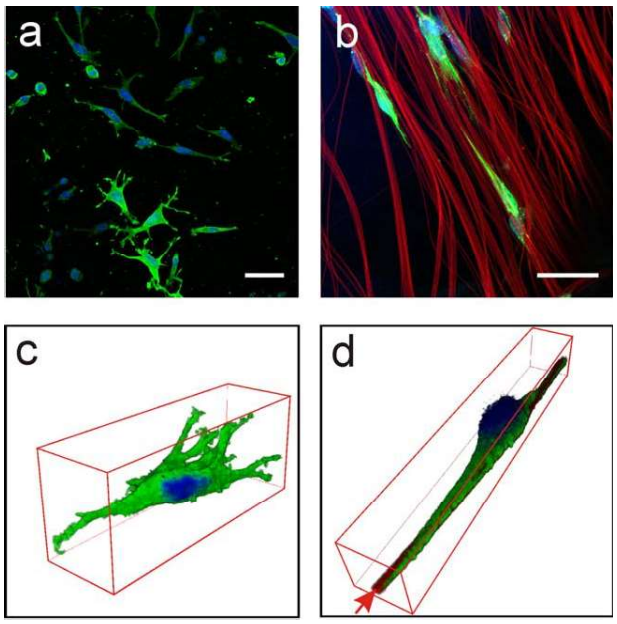

FIGURE 6. Gel-embedded PCL fibers affect cell morphology. To visualize the effects on cell shapes U373 cells were cultivated for 6 days in a 3D collagen matrix with and without PCL fibers. (a,b) Confocal microscopy images show immunostaining against S100 (green) and nuclear staining (DAPI, blue). PCL fibers were stained red using DiI. Panels (a) and (c) show cell morphologies in the absence of PCL fibers, panels (b) and (d) with PCL fibers in the gel. Different magnification are shown in (a) and (b) with all scale bars measuring 50 μm. (c,d) Reconstructions of cells from both conditions to display the different cellular morphology in space. The red arrow in (d) points at the PCL fiber. [Color figure can be viewed in the online issue, which is available at wileyonlinelibrary.com.]

arrays [Figure 5(c–e)]. The thickness of the gel layers between 3D fiber arrays was determined by the viscosity of the gel solution. To reduce displacement of the fibers by the collagen solution it was important to introduce them before gelation of the collagen took place. Gelation was initiated by heating the collagen to 37°C, but to some extent changes in viscosity of the collagen already occurred at room temperature. Thus with collagen gels we obtained a matrix with several 3D arrays of fibers separated by regions devoid of fibers [Figures 5(d) and 1(e)]. A standard array now consists of 10 layers of fibers and gels with a distance of 70–120 μm between the layers [Figure 5(e)]. An alternative method to contain the 3D fiber array within a hydrogel consisted in casting the gel solution over the fibers [Figure 5(f)].

The effect of fiber-containing collagen matrices on cell shape was first tested using the glial cell line U373. These cells grew well within the scaffolds and produced cellular processes. When the cells were cultivated inside the 3D collagen matrix without PCL fibers, we observed a more diverse morphology than in 2D cultures. In the 3D gels, many cells had complex cell bodies with several processes in various directions [Figure 6(a)]. When PCL fibers were added in 2D or 3D cultures cell bodies tended to attach to the polymer fibers [Figure 6(b)]. In 3D collagen matrices, all cells which made contact with PCL fibers produced only two processes pointing in opposing directions along the path of the PCL fiber. Additional processes could only be observed when cells had contact with more than one fiber. Despite their ability to grow in complex shapes within the 3D collagen gels [Figure 6(c)] the presence of PCL fibers imposed a fusiform morphology on the cells [Figure 6(d)].

Influence of PCL fibers on axonal growth

To assess the influence of the 3D gel/fiber substrates on Schwann cells and sensory neurons, DRG were explanted on the gels, and axonal growth and glial cell migration were quantified. Representative images of DRG cultures in collagen gels with and without PCL-fibers are shown in Figure 7. The 3D gel/fiber matrices caused a directional outgrowth of axons [Figure 7(a)] and a preference in the direction of cell migration [Figure 7(b)].

When comparing the total number of axonal endings we found no significant difference between the two conditions. Although initial neurite outgrowth was not influenced by the PCL fibers, this was the case for axonal elongation. Under control conditions, when no fibers were contained in the gel, the statistical analysis revealed no preference of axonal growth in any direction [Figures 7(a) and 8(a)]. At 4 DIV and 7 DIV the ratio of axon length in two orthogonal directions of the image was close to one [Figure 8(b)]. In contrast, collagen gels that contained aligned PCL-fibers had the effect that axons in direction of the PCL fibers were significantly longer than in the absence of fibers, and axons in the direction orthogonal to the PCL fibers were significantly shorter [Figure 8(a), t-test $p < 0.01$ at 4 DIV]. For instance, after 4 DIV mean axon lengths in parallel with PCL fibers was 1148 ± 81 μm, whereas in the orthogonal direction they only reached 378 ± 36 μm.

As axonal growth along the electrospun fibers continued in the cultures, the difference between the two directions was even larger at 7 DIV. Axons also continued to grow in collagen gels without PCL fibers. For this reason the difference in axon length between gels without PCL fibers and the preferred direction in the collagen/PCL fiber matrix was no longer significant. However, the orientation index demonstrated quantitatively that the fiber containing matrices continued to exert a strong guidance effect on the growing axons, whereas outgrowth was random in isotropic collagen gels [Figure 8(b)]. Comparing the results at both time points indicated that under all conditions axonal elongation slowed down during the time course of cultivation.

Influence of PCL fibers on glial cell migration

The data for cell migration demonstrated a similar effect of the aligned PCL fibers [Figures 7(b) and 8(c,d)]. Under the control condition of 3D gels without fibers there was no significant difference in the distance of cells that migrated from the DRG in vertical or horizontal direction (e.g., 4 DIV: 834 ± 52 μm vs. 780 ± 60 μm). When cultivated in the presence of aligned PCL-fibers, cell migration parallel to the fiber orientation reached significantly longer distances (e.g., at 4 DIV: 1509 ± 55 μm) in comparison with cell migration perpendicular to the PCL fibers (4 DIV, 7 DIV: both

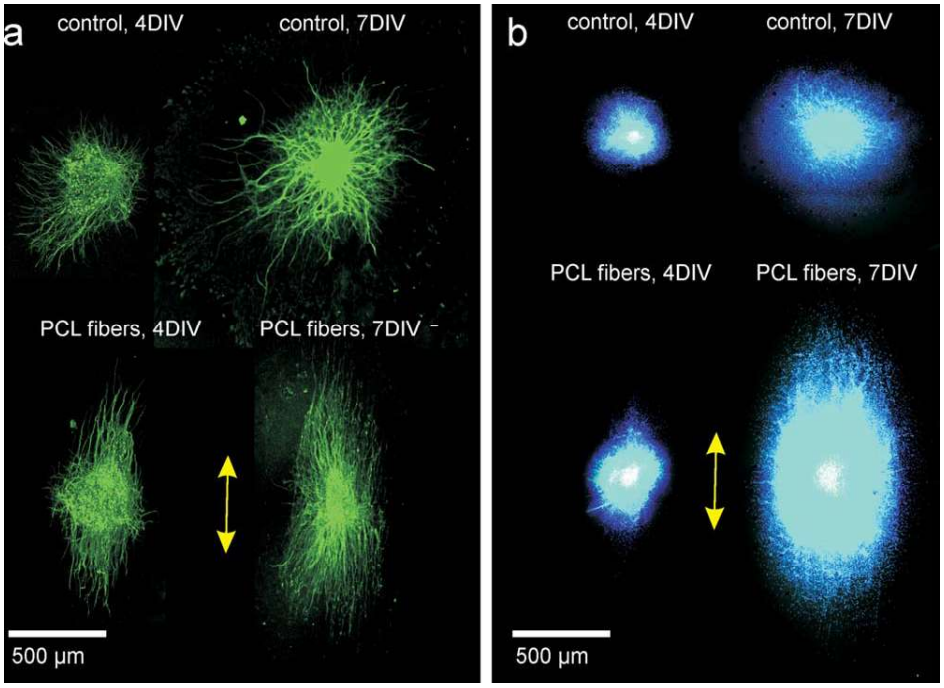

FIGURE 7. Gel-embedded PCL fibers as a guidance structure for Schwann cells and sensory neurons. Dorsal root ganglia were cultivated for 4 and 7 days in a 3D collagen matrix with and without PCL fibers as control. Axons were immunostained against NF200 (a) and nuclei were stained with DAPI (b). Yellow arrows indicate the orientation of PCL fibers in the samples. [Color figure can be viewed in the online issue, which is available at wileyonlinelibrary.com.]

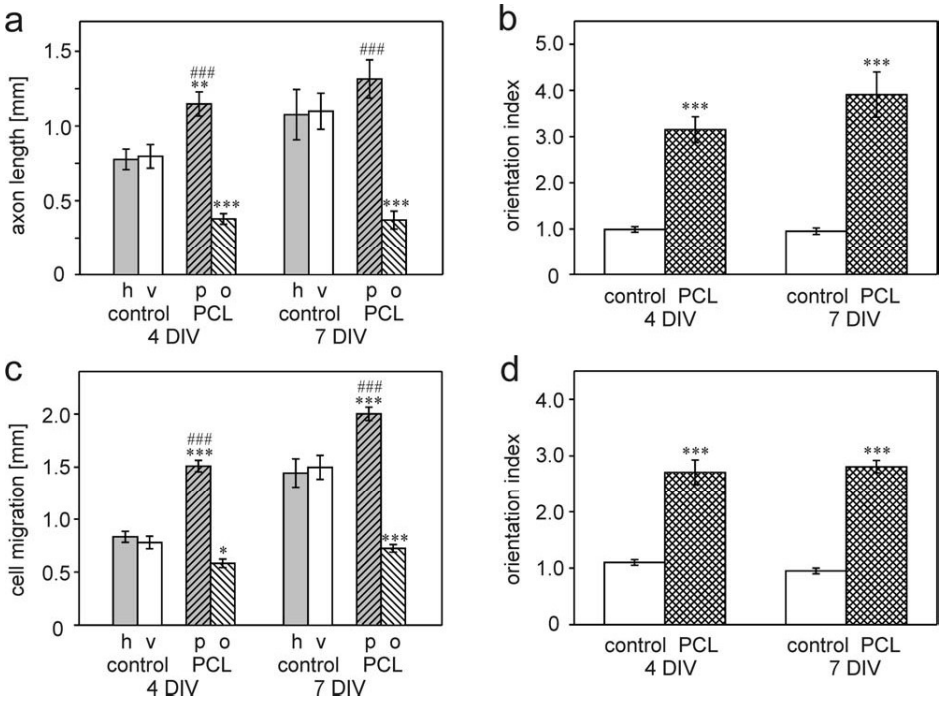

FIGURE 8. Quantification of the guidance properties of gel-embedded PCL fibres. (a) Axon length in different directions is plotted as a result of the different 3D substrates. Data show mean of the 10% longest axons of every explant. Substrates were collagen gels without or with PCL fibers. For the controls axonal growth was analyzed in arbitrarily defined horizontal and vertical (h and v) directions; for fiber containing gels axon lengths was assessed in parallel and orthogonal to the fiber direction (p and o). (b) An orientation index for axon length was determined as the ratio between the two directions measured for every condition (h/v or p/o). (c) The distance of cell migration from the DRG was quantified in a similar manner, and (d) an orientation index was calculated accordingly. Asterisks indicate significant differences between the PCL fiber sample and control; pound symbols indicate differences between the two directions within PCL fiber samples. Bars show mean ± SEM ($n \geq 6$ DRG explants; Student's *t*-test; $p^{*} < 0.05$; $p^{***} < 0.001$; $p^{\#\#\#} < 0.001$).

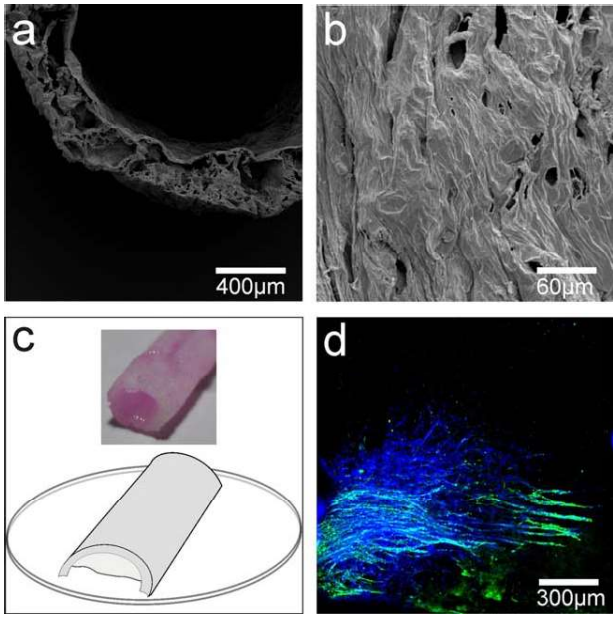

FIGURE 9. Integration of the composit scaffold into a biocompatible conduit. Conduits were produced from a mixture of a 12% PCL solution and NaCl by dipmolding and subsequent leaching of the NaCl fraction. (a,b) SEM images depict the porous structure of the conduits wall (cross-section in a) and surface (b). (c) Scheme of the culture model used to verify biocompatibility of the conduit. In the inset a photograph of the collagen-fiber scaffold integrated into the tubular PCL conduit is shown. (d) Axonal growth and cell migration occurred within the structured 3D conduit. Axons are marked with NF200 immunostaining, migrated cells with nuclear DAPI stain. [Color figure can be viewed in the online issue, which is available at wileyonlinelibrary.com.]

$p < 0.001$) and also in comparison with cell migration in 3D gels without fibers (4 DIV: $p < 0.05$; 7 DIV: $p < 0.001$). As for axonal growth the orientation index was highly significant at 4 DIV and 7 DIV [Figure 8(d)].

Incorporation of gel/fiber composites in a tubular conduit

To use the gel/fiber composite scaffold as a substrate for PN regeneration we inserted it into a PCL-conduit, which was manufactured by dip-coating a steel rod with PCL solution. The addition of NaCl to the PCL-solution and subsequent leaching resulted in the formation of a tubular conduit wall with a porous surface (Figure 9). It also increased the flexibility of the conduit and hence the suitability for *in vivo* applications. Surfaces and cross sections of tubes were examined with scanning electron microscopy [Figure 9(a,b)], and parameters of the dipping technique (concentration of the solutions, repetitions of coating) were adjusted according to the results.

PCL tubes were longitudinally cut in half, gel/fiber scaffolds were inserted into the half tubes, and artificial nerve bridges were then produced by sealing two half tubes with PCL-solution [Figure 9(c)]. To investigate the biocompatibility of the constructs, DRG explants were cultivated inside the half conduits, which were sealed with a cover slip, so that exchange of metabolic matter could only occur through the gel and PCL wall or via the endings of the conduit. The cultivated DRG showed no visible change in appearance compared with those cultivated in open 3D gels. After 7 DIV, axon growth and cell migration had occurred within the 3D matrix [Figure 9(d)] and on the surface of the cover slips. Anti-NF200 immunohistochemistry revealed widespread axonal growth and similar axon lengths to those observed in 3D cultures that were not enclosed by tubular conduits. Nuclear DAPI staining of cells that had migrated out of the DRG indicated cell migration was also not impaired.

DISCUSSION

To develop artificial scaffolds for PN regeneration we have described a method for the 3D assembly of electrospun PCL fibers in parallel alignment. Consecutive embedding of these fibers in layers of collagen gels and incorporation in a tubular conduit resulted in a 3D scaffold for axonal guidance, whose biological use was tested with DRG explants. Schwann cells and sensory axons adhered to the PCL fiber substrate and were guided by the orientated structure inside the gel/fiber scaffold. Within the 3D collagen gels contact with the microfibers caused the cells to assume a spindle-shaped morphology following the fiber direction.

Previous developments of fiber substrates revealed two major challenges with respect to the goal of an artificial nerve implant, (1) the incorporation of microfibers in a 3D configuration, and (2) the functionalization of the growth substrate to attract axonal gowth over long distances.[17] The present study contributes to solving the first of these problems and provides a 3D platform to address the second.

Three-dimensional configuration of guidance structures

Artificial nerve bridges are designed as tubular grafts that connect the proximal with the distal PN stump.[3,4] When hollow cylinders with a single lumen are used, regenerating axons and migrating cells accumulate on the inside of the tubular walls. Constructs with several lumens were fabricated to increase that surface area and to separate different fiber bundles within the conduit.[6,7,20] However, increasing the number of compartments with these methods, for example by using seven channels or by incorporating three films, did not improve regeneration.[6,7] Although implants have also been developed that were filled with non-orientated "isotropic" matrices,[21–24] most studies indicate that orientated 3D structures with a large surface area are required to provide an adequate substrate for long distance axonal guidance.[4,5] We can distinguish two basic designs that provide such internal guidance structures within tubular implants (Figure 1): The tubes contain either longitudinal fibers or a porous matrix with longitudinal orientation of the pores. Conduits that consist of polymer fibers can be produced by a number of different techniques such as drawing from a melt, template synthesis, phase separation, self assembly and electrospinning.[12–14] A major challenge consists in filling the conduit with the orientated fibers.

One strategy consists of stacking 2D films of parallel fibers above one another. In one previous study, this was done with 10–12 films of electrospun poly(acrylonitrile-co-methylacrylate) fibers inside longitudinally split polysulfone

tubes, which were then sealed and implanted to bridge 17 mm sciatic nerve gaps in rats.[14] More recently, an improved method for manufacturing 3D fiber scaffolds was published.[25] Highly aligned parallel fibers were electrospun onto individual non-conductive frames using a conductive wire as target. The holding frames with suspended microfibers were then placed across the surface of a hydrogel, covered with a spacer frame and another layer of hydrogel was added. This process was repeated several times to create a 3D microfiber scaffold.[25] Our procedure explained in the present paper is based on the 3D accumulation of fibers already during the spinning process. This could be used also for successive stacking of fiber and gel layers [Figure 5(d,e)] or for casting a gel over the 3D fiber array [Figure 5(f)].

While we modified the physical design of the target electrode to achieve a 3D fiber configuration, a similar technique of "air gap electrospinning" also used two horizontally separated targets, each connected to a common voltage with respect to the spinneret.[19] To manufacture an implantable scaffold, an exterior coating of poly(glycolic acid)/poly(lactic acid) copolymer was in this case deposited onto the outside of the cylindrical fiber configuration. For this, a circular steel plate was placed behind the fibers, and the spinneret was used for subsequent electrospraying of the copolymer.[19] A different technique was developed by Schlosshauer's group, who fabricated oriented PCL filaments by hot melt extrusion through nozzles with six-leaf cross sections. After extrusion, the filaments were drawn in a separate process. This resulted in yarns of several hundred filaments, each with six longitudinal grooves, which could be inserted in a tubular conduit.[10] These structured filaments have been functionalized in various ways including siRNA[26] and were successfully used to fill epineurial tubes *in vivo*.[27] Using the method of injection molding chitosan conduits were produced that contained several hundreds of longitudinally aligned PLGA fibers.[28,29]

The second approach to achieve internally structured implants aims at scaffolds with longitudinal pores or channels. One method to achieve this is the application of strong magnetic fields which orient collagen or fibrin matrices.[8,30,31] Another promising technique consists in the controlled freeze drying of collagen suspensions. When the solvent is caused to freeze from one side of the solution, collagen is displaced, thus resulting in collagen walls of longitudinally orientated guidance channels. The diameter of these pores can be controlled to be in the range of 20–120 μm.[9,32,33] Structured collagen conduits, which are commercially available (Perimaix, Matricel GmbH), were implanted as sciatic nerve grafts in rats, and axonal regeneration followed the longitudinal pores of the artificial nerve guide. In these experiments better outcomes were achieved by co-implanting Schwann cells,[34] though fiber containing implants appear to achieve similar or better results without the need to implant live cells.[28,35]

Biological functionalization of the growth substrate

Although pure polymer fibers, such as PCL or poly(lactic acid), already proved useful as guidance structures, several studies showed that functionalization either by covalent binding of ECM peptides[17] or blending with ECM proteins[13] improved the ability of such fibers to guide cell migration and axonal growth. In the present experiments the surrounding gel already consisted of collagen with signal sequences that can activate cellular integrin receptors. With the use of hydrogels that contain signaling molecules one might therefore use artificial polymer fibers without the further need of functionalization. We found that axonal growth along non-functionalized PCL fibers in a 3D collagen environment was initially faster than in pure collagen, however, with time, that is after 1 wk, this difference disappeared. Possibly, activation of axonal integrin receptors by the collagen supported axonal elongation whereas no such signaling was initiated by the PCL. This outcome suggests that additional modification of the fibers with signaling molecules may be beneficial.

Coating of artificial polymer fibers with laminin or fibronectin enabled axons to grow faster than the migration of Schwann cells.[5] An easy technique to achieve such functionalization consists of blending a synthetic polymer with fibronectin, collagen or laminin when preparing the electrospinning solution. Cell culture investigations demonstrated this approach to be even superior to more sophisticated chemical modification.[36] Recently, an innovative method for the synthesis of covalently functionalized poly(D,L-lactide-co-glycolide) fibers has been published. The polyester were made hydrophilic by adding star-shaped poly(ethylene oxide) followed by covalent binding of cell-adhesion-mediating peptides. The resulting fiber matrix was bioactive and promoted cell adhesion via recognition of the immobilized binding motifs.[37] For functionalization through blending or covalent modification in the electrospinning solution the present 3D spinning setup with step targets can be used without further modifications.

When, as here, electrospun fibers are embedded in a biocompatible hydrogel, the preferential adherence of axons to the electrospun fibers is an issue. In previous 2D studies aligned fibers were placed on non-treated tissue culture plastic[14] or on cell repellent substrates,[13,15] which left the cells little choice but to attach to the fiber substrate. In 3D composites that consist of guidance fibers suspended in a supportive matrix a suitable balance of cell surface attachment between the different material components must be struck. With the imbedding of pure PCL fibers in a collagen gel the guidance effect or the morphological alignment was maintained. It remains to be seen whether this remains when additional growth promoting factors, for example neurotrophins, are introduced into the matrix.[1] Different combinations of gels and modification of artificial polymers can now be tested.

CONCLUSION

We report a technique for the 3D electrospinning of parallel microfibers that were suspended in collagen gels and incorporated in a tubular nerve implant. In contrast to conventional hollow nerve conduits, this nerve guide with aligned arrays of anisotropic fibers directed axonal regeneration and

Schwann cell migration in the longitudinal axis of the scaffold. The comparative advantage of this design in comparison with alternative designs will now be tested *in vivo*.

REFERENCES

1. Dalton PD, Mey J. Neural interactions with materials. Front Biosci 2009;14:769–795.
2. Deumens R, Bozkurt A, Meek MF, Marcus MAE, Joosten EAJ, Weis J, Brook GA. Repairing injured peripheral nerve bridges: Bridging the gap. Prog Neurobiol 2010;92:245–276.
3. Siemionow M, Bozkurt M, Zor F. Regeneration and repair of peripheral nerves with different biomaterials: A review. Microsurgery 2010;30:574–588.
4. Mey J, Brook G, Hodde D, Kriebel A. Electrospun fibers as substrates for peripheral nerve regeneration. Adv Polym Sci 2012;246:131–170.
5. Hoffman-Kim D, Mitchel JA, Bellamkonda RV. Topography, cell response, and nerve regeneration. Annu Rev Biomed Eng 2010; 12:203–231.
6. Clements IP, Kim Y-T, English AW, Lu X, Chung A, Bellamkonda RV. Thin-film enhanced nerve guidance channels for peripheral nerve repair. Biomaterials 2009;30:3834–3846.
7. Yao L, de Ruiter GC, Wang H, Knight AM, Spinner RJ, Yaszemski MJ, Windebank AJ, Pandit A. Controlling dispersion of axonal regeneration using a multichannel collagen nerve conduit. Biomaterials 2010;31:5789–5797.
8. Ceballos D, Navarro X, Dubey N, Wendelschafer-Crabb G, Kennedy WR, Tranquillo RT. Magnetically aligned collagen gel filling a collagen nerve guide improves peripheral nerve regeneration. Exp Neurol 1999;158:290–300.
9. Möllers S, Heschel I, Damink LH, Schugner F, Deumens R, Muller B, Bozkurt A, Nava JG, Noth J, Brook GA. Cytocompatibility of a novel, longitudinally microstructured collagen scaffold intended for nerve tissue repair. Tissue Eng Part A 2009;15:461–472.
10. Ribeiro-Resende VT, Koenig B, Nichterwitz S, Oberhoffner S, Schlosshauer B. Strategies for inducing the formation of bands of Bungner in peripheral nerve regeneration. Biomaterials 2009;30: 5251–5259.
11. Matsumoto K, Ohnishi K, Kiyotani T, Sekine T, Eng HUM, Nakamura T, Endo K, Shimizu Y. Peripheral nerve regeneration across an 80-mm gap bridged by a polyglycolic acid (PGA)-collagen tube filled with laminin-coated collagen fibers: A histological and electrophysiological evaluation of regenerated nerves. Brain Res 2000;868:315–328.
12. Teo WE, Ramakrishna S. A review on electrospinning design and nanofibre assemblies. Nanotechnology 2006;17:89–106.
13. Schnell E, Klinkhammer K, Balzer S, Brook GA, Klee D, Dalton PD, Mey J. Guidance of glial cell migration and axonal growth on electrospun nanofibers of poly-å-caprolactone and a collagen/poly-å-caprolactone blend. Biomaterials 2007;28:3012–3025.
14. Kim YT, Haftel VK, Kumar S, Bellamkonda RV. The role of aligned polymer fiber-based constructs in the bridging of long peripheral nerve gaps. Biomaterials 2008;29:3117–3127.
15. Klinkhammer K, Seiler N, Grafahrend D, Mey J, Brook GA, Möller M, Dalton PD, Klee D. Deposition of electrospun fibers on reactive substrates for in vitro investigation. Tissue Eng 2009;15:77–85.
16. Gerardo-Nava J, Führmann T, Klinkhammer K, Seiler N, Mey J, Klee D, Möller M, Dalton PD, Brook GA. Human neural and glial interactions with electrospun nanofibres in vitro. Nanomedicine 2008;4:11–30.
17. Bockelmann J, Klinkhammer K, von HA, Seiler N, Faissner A, Brook GA, Klee D, Mey J. Functionalization of electrospun poly(epsilon-caprolactone) fibers with the extracellular matrix-derived peptide GRGDS improves guidance of Schwann cell migration and axonal growth. Tissue Eng Part A 2011;17:475–486.
18. Chang C-J. Effects of nerve growth factor from genepin-crosslinked genepin in polycaprolactone conduit on peripheral nerve regeneration—*in vitro* and *in vivo*. J Biomed Mater Res A 2008;91:586–596.
19. Jha BS, Colello RJ, Bowman JR, Sell SA, Lee KD, Bigbee JW, Bowlin GL, Chow WN, Mathern BE, Simpson DG. Two pole air gap electrospinning: Fabrication of highly aligned, three-dimensional scaffolds for nerve reconstruction. Acta Biomater 2011;7:203–215.
20. de Ruiter GC, Spinner RJ, Malessy MJ, Moore MJ, Sorenson EJ, Currier BL, Yaszemski MJ, Windebank AJ. Accuracy of motor axon regeneration across autograft, single-lumen, and multichannel poly(lactic-co-glycolic acid) nerve tubes. Neurosurgery 2008; 63:144–153.
21. Labrador RO, Buti M, Navarro X. Influence of collagen and laminin gels concentration on nerve regeneration after resection and tube repair. Exp Neurol 1998;149:243–252.
22. Toba T, Nakamura T, Shimizu Y, Matsumoto K, Ohnishi K, Fukuda S, Yoshitani M, Ueda H, Hori Y, Endo K. Regeneration of canine peroneal nerve with the use of a polyglycolic acid-collagen tube filled with laminin-soaked collagen sponge: A comparative study of collagen sponge and collagen fibers as filling materials for nerve conduits. J Biomed Mater Res 2001;58:622–630.
23. Inada Y, Morimoto S, Takakura Y, Nakamura T. Regeneration of peripheral nerve gaps with a polyglycolic acid-collagen tube. Neurosurgery 2004;55:640–646.
24. McGrath AM, Novikova LN, Novikov LN, Wiberg M. BD™ PuraMatrix™ peptide hydrogel seeded with Schwann cells for peripheral nerve regeneration. Brain Res Bull 2010;83:207–213.
25. Yang Y, Wimpenny I, Ahearne M. Portable nanofiber meshes dictate cell orientation throughout three dimensional hydrogels. Nanomedicine 2011;7:131–136.
26. Hoffmann N, Mittnacht U, Hartmann H, Baumer Y, Kjems J, Oberhoffner S, Schlosshauer B. Neuronal and glial responses to siRNA-coated nerve guide implants in vitro. Neurosci Lett 2011; 494:14–18.
27. Hajosch R, Grupp L, Nichterwitz S, Schlosshauer B. A novel microsurgical nerve implantation technique preserving outer nerve layers. J Neurosci Methods 2010;189:205–209.
28. Wang X, Hu W, Cao Y, Yao J, Hu J, Gu X. Dog sciatic nerve regeneration across 30 mm defect bridged by a chitosan/PGA artificial nerve graft. Brain 2005;128:1897–1910.
29. Ding F, Wu J, Yang Y, Hu W, Zhu Q, Tang X, Liu J, Gu X. Use of tissue-engineered nerve grafts consisting of a chitosan/poly(lactic-co-glycolic acid)-based scaffold included with bone marrow mesenchymal cells for bridging 50-mm dog sciatic nerve gaps. Tissue Eng Part A 2010;16:3779–3790.
30. Dubey N, Letourneau PC, Tranquillo RT. Guided neurite elongation and Schwann cell invasion into magnetically aligned collagen in simulated peripheral nerve regeneration. Exp Neurol 1999;158: 338–350.
31. Verdu E, Labrador RO, Rodriguez FJ, Ceballos D, Fores J, Navarro X. Alignment of collagen and laminin-containing gels improves nerve regeneration within silicone tubes. Restor Neurol Neurosci 2002;20:169–179.
32. Bozkurt A, Brook GA, Moellers S, Lassner F, Sellhaus B, Weis J, Woeltje M, Tank J, Beckmann C, Fuchs P, Damink LO, Schügner F, Heschel I, Pallua N. In vitro assessment of axonal growth using dorsal root ganglia explants in a novel three-dimensional collagen matrix. Tissue Eng 2007;13:2971–2979.
33. Bozkurt A, Deumens R, Beckmann C, Olde Damink L, Schugner F, Heschel I, Sellhaus B, Weis J, Jahnen-Dechent W, Brook GA, Pallua N. In vitro cell alignment obtained with a Schwann cell enriched microstructured nerve guide with longitudinal guidance channels. Biomaterials 2009;30:169–179.
34. Bozkurt A, Lassner F, O'Dey D, Deumens R, Bocker A, Schwendt T, Janzen C, Suschek CV, Tolba R, Kobayashi E, Sellhaus B, Tholl S, Eummelen L, Schügner F, Damink LO, Weis J, Brook GA, Pallua N. The role of microstructured and interconnected pore channels in a collagen-based nerve guide on axonal regeneration in peripheral nerves. Biomaterials 2012;33:1363–1375.
35. Hu N, Wu H, Xue C, Gong Y, Wu J, Xiao Z, Yang Y, Ding F, Gu X. Long-term outcome of the repair of 50 mm long median nerve defects in rhesus monkeys with marrow mesenchymal stem cells-containing, chitosan-based tissue engineered nerve grafts. Biomaterials 2013;34:100–111.
36. Koh HS, Yong T, Chan CK, Ramakrishna S. Enhancement of neurite outgrowth using nano-structured scaffolds coupled with laminin. Biomaterials 2008;29:3574–3582.
37. Grafahrend D, Heffels KH, Beer MV, Gasteier P, Moller M, Boehm G, Dalton PD, Groll J. Degradable polyester scaffolds with controlled surface chemistry combining minimal protein adsorption with specific bioactivation. Nat Mater 2011;10:67–73.